Journal of Thermal Analysis and Calorimetry, Vol. 72 (2003) 231–239

PHASE DIAGRAM AND ELECTRICAL CONDUCTIVITY OF $TbBr_3$–NaBr BINARY SYSTEM

L. Rycerz[1*], *M. Cieślak-Golonka*[1], *E. Ingier-Stocka*[1] *and M. Gaune-Escard*[2]

[1]Institute of Inorganic Chemistry and Metallurgy of Rare Elements, Wrocław University of Technology, Wybrzeze Wyspianskiego 27, 50-370 Wrocław, Poland
[2]Ecole Polytechnique, Mécanique & Energétique, Technopole de Château-Gombert, 5 rue Enrico Fermi, 13453 Marseille Cedex 13, France

Abstract

Several experimental techniques were used to characterise the physicochemical properties of the $TbBr_3$–NaBr system. The phase diagram determined by DSC, exhibits an eutectic and a Na_3TbBr_6 stoichiometric compound that decomposes peritectically (759 K) shortly after a solid–solid phase transition (745 K). The eutectic composition, $x(TbBr_3)$=39.5 mol%, was obtained from the Tamman method. This mixture melts at 699 K. With the corresponding enthalpy of about 16.1 kJ mol^{-1}. Diffuse reflectance spectra of the pure components and their solid mixtures (after homogenisation in the liquid state) confirmed the existence of new phase exhibiting its own spectral characteristics, which may be possibly related to the formation of Na_3TbBr_6 in this system. Additionally, the electrical conductivity of $TbBr_3$–NaBr liquid mixtures was measured down to temperatures below solidification over the whole composition range.

Keywords: differential scanning calorimetry, electrical conductivity, phase diagram, sodium bromide, terbium(III) bromide

Introduction

Rare earths play a significant role in everyday life and in sophisticated industrial applications. They are extracted and processed into metals, magnet alloys oxides and other forms. Extraction and processing of lanthanide are largely based on molten salt technologies. Many processes are still under development; particularly those dealing with reprocessing of spent nuclear fuel or nuclear waste processing [1–2] or metal halide lamps [3]. However data on lanthanide compounds are scarce and not easily accessible in literature. As a consequence, intensive efforts are made at an international level both on the research and development aspects and also on data bank development [4].

The present work is a continuation of systematic investigations of thermodynamic, structural and electrical properties of lanthanide halide systems by a variety of

* Author for correspondence: E-mail: ingier@ichn.ch.pwr.wroc.pl

1388–6150/2003/ $ 20.00
Akadémiai Kiadó, Budapest

experimental techniques, such as calorimetry [5–21], electrical conductivity and density measurements [22–24], X-ray and neutron diffraction [25–27]. Numerical procedures, based on theoretical approaches of ionic interactions in these trivalent halide melts [28], were also used to calculate phase equilibria or structural features by molecular dynamic simulations [10, 29–30].

Experimental

Terbium bromide, $TbBr_3$, was prepared by sintering bromination of terbium oxide Tb_4O_7 (Johnson Matthey, 99.9%) with ammonium bromide NH_4Br (POCh Gliwice, Poland). The terbium oxide–ammonium bromide mixture (molar ratio=1:14) was heated slowly up to 570 K. After 3 h reaction at 570 K, temperature was increased up to 650 K, nonreacted ammonium bromide was sublimated. Finally the salt was melted at 1150 K, cooled and transferred to the glove box. Further purification of crude terbium bromide was obtained by distillation under reduced pressure (~0.1 Pa) at 1170 K.

The chemical analysis of the synthesised $TbBr_3$ was performed by titration methods for bromide (mercurimetric) and lanthanide (complexometric). These results are presented in Table 1.

Table 1 Chemical analysis of terbium tribromide

Compound	$Br_{experimental}$/	$Br_{theoretical}$/	$Tb_{experimental}$/	$Tb_{theoretical}$/
	mass%			
$TbBr_3$	60.15	60.13	39.85	39.87

Sodium bromide was Merck Suprapur reagent (min. 99.9%). Prior to use, it was progressively heated up to fusion under gaseous HBr atmosphere. HBr in excess was then removed from the melt by argon bubbling.

The mixtures of $TbBr_3$ and NaBr (in appropriate proportions) were melted in vacuum-sealed quartz ampoules in an electric furnace. Melts were homogenised by shaking and solidified. These samples were ground in an agate mortar in a glove box. Homogeneous mixtures of different composition prepared along the same procedure were used in phase diagram and electrical conductivity measurements.

All chemicals were handled in an argon glove box with a measured volume fraction of water of about $2 \cdot 10^{-6}$ and continuous gas purification by forced recirculation through external molecular sieves.

A Setaram DSC 121 differential scanning calorimeter (DSC) (150–1100 K) was used for the determination of the temperature and enthalpy of phase transitions. Samples (300–500 mg) were contained in vacuum-sealed quartz ampoules (about 6 mm diameter, 15 mm length). The side walls of ampoules were grounded in order to fit the cells snugly into the heat flow detector. The DSC experiments were conducted at heating and cooling rates between 1 and 5 K min^{-1} on samples with 22 compositions.

Electrical conductivity measurements were carried out in capillary quartz cell described in details elsewhere [31]. The cell filled with the compound under investigation was placed into a furnace with a stainless steel block, used to achieve a uniform temperature distribution. The conductivity of the melt was measured by platinum electrodes with conductivity meter Tacussel CD 810. Experimental runs were conducted both upon heating and cooling regimes at rates ranging 1–2 K min^{-1}. The mean value of these two measurements was used in calculations. Temperature and conductivity data acquisition was made with a PC interfaced to the conductivity meter. The accuracy of electrical conductivity measurements was estimated at ±2%. Temperature was measured by means of a Pt/Pt–Rh thermocouple within the accuracy 1 K. Experimental cell was calibrated with a pure NaCl melt [32]. The resulting cell constant was 152 cm^{-1}. The same cell was used for all experiments and the cell constant checked from time to time in order to control any possible evolution. These measurements were carried out under static argon atmosphere.

Electronic reflectance spectra of powdered samples were measured with a Carry 500 Scan UV-Vis-NIR spectrophotometer (Varian) in the 8 000–50 000 cm^{-1} range. The scan rate was 3614 cm^{-1} min^{-1}, data interval 1 nm, slit width 2 nm.

Results and discussion

$TbBr_3$–NaBr phase diagram was established for the first time in the course of the present work. DSC investigations performed on samples with 22 compositions yielded both the temperature and the fusion enthalpy of the concerned mixtures. The values of enthalpies of thermal effects obtained from heating and cooling curves were almost the same, the difference between them being no more than 2%. However, supercooling was observed on cooling curves. Due to this supercooling effect, all values of temperature and enthalpy given in this work were determined from the heating curves.

Temperature and enthalpy of fusion of pure $TbBr_3$ were determined separately by high temperature Calvet microcalorimetry because of the temperature limitation of DSC. It was found that fusion occurs at 1103 K with the corresponding enthalpy of 37.4 kJ mol^{-1}. The results obtained are in excellent agreement with literature data giving the same temperature of fusion and enthalpy of 37.7 kJ mol^{-1} [33].

The phase diagram of the system under investigation was found to be peritectic type. In the range of about 30–100 mol% of $TbBr_3$, only two peaks ascribed to the eutectic and the liquidus effects were found in every DSC curve. The thermal effect related to the eutectic phase disappears at compositions equal or less than 25 mol%. The eutectic contribution to the enthalpy of fusion was determined and plotted against the composition in Fig. 1. This so-called Tamman construction makes it possible to evaluate accurately the eutectic composition from the intercept of the two linear parts in Fig. 1, described by the equations $\Delta_{fus}H^0_m = -27.79 + 1.11x(TbBr_3)$ and $\Delta_{fus}H^0_m = 26.59 - 0.266x(TbBr_3)$ in kJ mol^{-1}, respectively. In these equations, $x(TbBr_3)$ denotes the molar concentration (mol%) of terbium tribromide. We obtained $x(TbBr_3)$= 39.5 mol% as the eutectic composition while the eutectic temperature de-

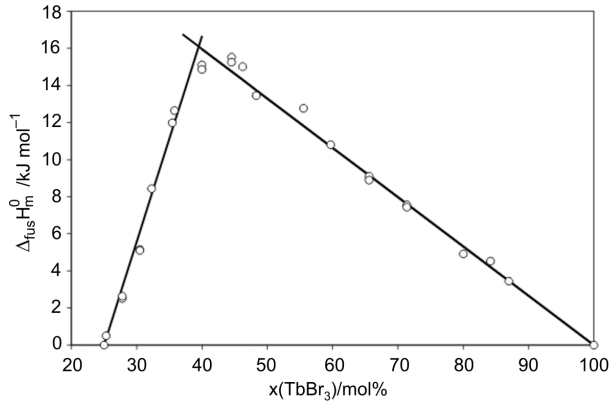

Fig. 1 Tamman diagram of $TbBr_3$–NaBr system (determination of the eutectic composition)

termined from all the appropriate DSC curves is T_{eut}=699 K. The enthalpy of fusion at the eutectic composition is $\Delta_{fus}H^0_m$=16.1 kJ mol^{-1}. In this Tamman construction it was assumed that there was no solubility in the solid state. Thus straight lines intercept the composition axis at $x(TbBr_3)$=25.0 mol% and $x(TbBr_3)$=100 mol%.

The examination of the DSC curves in the composition range $0<x(TbBr_3)<30$ mol% suggests that in this area the stoichiometric compound exists up to T=759 K, temperature at which it decomposes peritectically. The experimental composition $x(TbBr_3)$= 24.94 mol%, determined from a Tamman construction (Fig. 2), argues well with the Na_3TbBr_6 stoichiometry. The thermal effect that is visible in all DSC curves corresponds either to a phase transition in this compound or to its formation, as observed for other M_3LnCl_6 compounds that form at high temperature and then undergo congruent or incongruent melting.

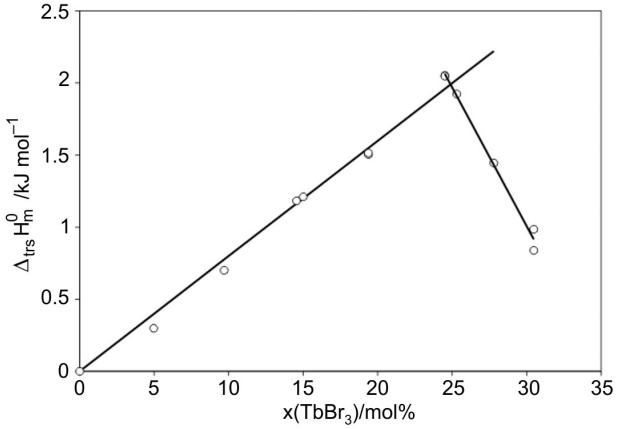

Fig. 2 Tamman diagram of $TbBr_3$–NaBr system (determination of the peritectic compound composition)

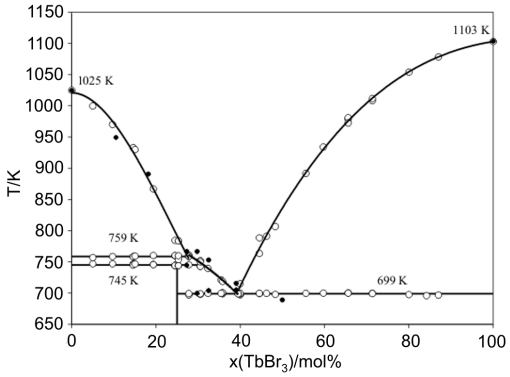

Fig. 3 Phase diagram of $TbBr_3$–NaBr system; o – DSC method; ● – electric conductivity method

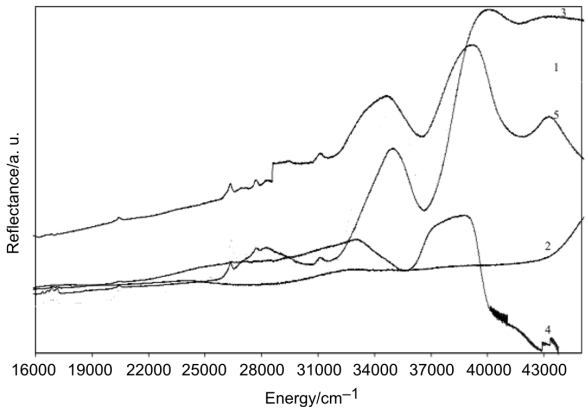

Fig. 4 Reflectance spectra of powdered samples: 1– the pure $TbBr_3$; 2 – NaBr; 3 – the simple mixture of 10 mol% $TbBr_3$ and 90 mol% NaBr; 4 – the mixture of 10 mol% $TbBr_3$ and 90 mol% NaBr after melting; 5 – the melting product(s) of 57.6 mol% $TbBr_3$ and 42.4 mol% NaBr

The complete phase diagram of $TbBr_3$–NaBr binary system is presented in Fig. 3.

In order to confirm the formation of new phase in this system, the diffuse reflectance spectra were investigated for several mixtures of $TbBr_3$ and NaBr. The reflectance spectra of powdered pure $TbBr_3$ (**1**), NaBr (**2**), a simple mechanical mixture of 10 mol% of $TbBr_3$ and 90 mol% of NaBr (**3**), similar mixture but after melting, cooling and powdering of the salts (**4**) and the melting product of 57.6 mol% of $TbBr_3$ and 42.4 mol% of NaBr (**5**) are presented in Fig. 4. The comparison of spectrum (**1**) and (**3**) shows only slight change in resolution between pure terbium bromide and the same salt but dilute in NaBr matrix. Practically, (**3**) is electronic spectrum of $TbBr_3$ less resolved upon dilution with its clear division between narrow, low intensity f–f bands of Tb^{3+} up to ca 32 000 cm^{-1} (ground state $^7F_6$) and broader, high intensity ligand-to-metal charge transfer bands ($\pi Br \rightarrow Tb^{3+}$) at 34 000 and 39 000 cm^{-1}. The latter bands are easily identifiable as π bands as for example, the position of that of

lowest energy taken to the Jorgensen formulae [34] for optical electronegativity give χ=1.7 for terbium(III), in agreement with the χ values for other lanthanide ions.

However, the comparison of spectra (**3**) and (**4**) shows the dramatic change of the latter, i.e. the spectrum of the salts mixture after melting. Generally, in (**4**) the f–f region is very weakly resolved, and in the CT region two broad asymmetric, bathochromically shifted bands at 33 000 and 38 000 cm^{-1} are seen. The most interesting is that the intensity of its higher energy branch is sharply going down, untypically both for pure $TbBr_3$ (**1**) and that of sodium bromide (**2**) (Fig. 4). Thus, practically, in (**4**) the 40 000–50 000 cm^{-1} region is 'empty' except the weak band at 44 000 cm^{-1} which is best seen for (**5**).

The spectrum of 25 mol% $TbBr_3$–75 mol% NaBr mixture after melting and solidification (not shown for the clarity) is similar to (**4**). However, when the mixture consists of 57.6 mol% of $TbBr_3$ and 42.4 mol% of NaBr (**5**) we have another picture: the clear bands at 34 000 and 39 000 cm^{-1}, characteristic of $TbBr_3$, and one well resolved additional band at 43 000 cm^{-1}.

The tentative explanation of the results presented in Fig. 4 can be as follows. It is clear that upon melting of the mixtures containing 10 and 25 mol% of $TbBr_3$ a new phase is formed. This phase has different spectral characteristic (**4**). Most probably, NaBr has been consumed at least partly, since spectra (**4**) and (**5**) show decreasing absorptivity in higher energy region, in contrast to NaBr (**2**). At higher $TbBr_3$ contents, this compound can be most probable a component of the system, which may contain also a new component, formed earlier (**4**), which bands are overlapped by the strong bands of $TbBr_3$.

This tentative interpretation of reflectance spectra is in excellent agreement with the phase diagram presented in Fig. 3. At the composition $x(TbBr_3)$=25 mol%, the

Table 2 Specific conductivity κ/S cm^{-1} of $TbBr_3$–NaBr melts

x_{TbBr3}/ mol%	$\kappa = A + BT + CT^2$			Temp. range/K
	A	10^3 B	10^7 C	
0	–7.8904	18.134	–73.583	1028–1120
10.49	–3.4510	8.6363	–31.195	949–1084
18.12	–2.2971	5.7641	–22.943	890–1080
29.72	–1.9528	5.2686	–23.023	767–890
32.44	–1.8959	4.6001	–16.266	751–885
39.02	–1.4097	3.2216	–7.1843	717–887
49.97	–1.2082	2.7716	–5.1453	713–978
59.72	–1.3799	2.8645	–6.5761	865–1028
70.26	–8.2725	15.209	–62.827	1057–1128
100	–3.6130	6.0590	–21.291	1104–1170

only existing phase is the Na_3TbBr_6 compound. At compositions $x(TbBr_3)$<25 mol% this compound coexists with NaBr, whereas at compositions $x(TbBr_3)$>25 mol%, it coexists with $TbBr_3$. It also illustrates that bands of $TbBr_3$ are visible in reflectance spectrum (**5**) while they are not visible in spectrum (**4**).

Therefore it is now clear that the thermal effect at 745 K, previously observed by DSC in samples of compositions $x(TbBr_3)$=0.25, does not correspond to the formation of the Na_3TbBr_6 compound. It is likely that this compound already exists at lower temperatures and that the enthalpy change at 745 K ($\Delta_{trs}H^0_m$=10.6 kJ mol^{-1}) corresponds to a phase transition. Structural investigations are in project and will provide characterisation of the low and high temperature phases. The latters exists on a narrow temperature range since Na_3TbBr_6 decomposes peritectically at T=759 K.

Electrical conductivity measurements were performed complementarily on the $TbBr_3$–NaBr system. The data obtained are original since neither $TbBr_3$ nor the $TbBr_3$–NaBr mixtures had been investigated previously. Measurements were performed over the entire composition range by increments of ~10 mol%. The main goal was to investigate the conductance of the liquid phase. However, the solid phase was also examined at some compositions for the purpose of correlating the characteristic temperatures determined by DSC to those observed with this new technique. These two sets are consistent as evidenced in Fig. 3.

As it can be seen a quite good compatibility was obtained. The fusion temperatures determined were as follows: $T_{fus}(TbBr_3)$=1103 K (Calvet microcalorimetry) and 1104 K (cond.); T_{fus}(NaBr)=1025 K (DSC) and 1012 K (cond.); T_{fus}(~40 mol% $TbBr_3$)=700 K (DSC) and 705 K (cond.). The same similarity was with the liquidus temperatures, e.g. $T_{liquidus}$(~39 mol% $TbBr_3$)=715 K (DSC) and 717 K (cond.).

The specific conductivity data of the liquid phase were fitted by polynomial Eq. (1):

$$\kappa = A + BT + CT^2 \quad (1)$$

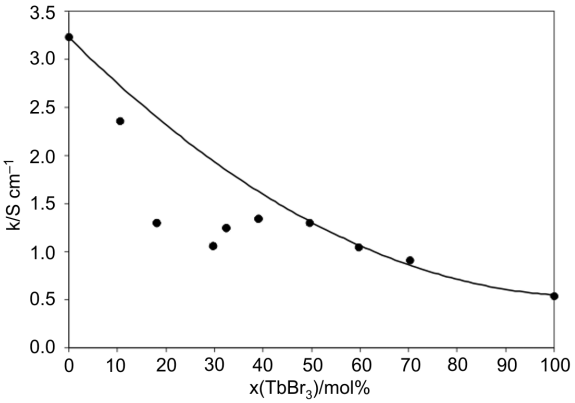

Fig. 5 Specific conductivity of $TbBr_3$–NaBr mixtures at 1150 K

The coefficients of equation are listed in Table 2. The specific conductivity dependence on composition at temperature 1150 K is shown in Fig. 5. Generally, the specific conductance decreases with increasing of $TbBr_3$ concentration. Moreover the results point out a deep minimum at ~25 mol% $TbBr_3$ what correlates well with the calorimetric measurements and suggests formation of the complex anion $TbBr_6^{3-}$.

Conclusions

The investigations of the $TbBr_3$–NaBr system carried out by three methods (DSC, electrical conductivity and spectroscopy) made it possible to construct a phase diagram of the system. The conductivity and spectroscopy as the subsidiary methods proved to be proper to confirm the results obtained by DSC. It was revealed that only one compound Na_3TbBr_6 exists in the system under investigation. It undergoes a solid–solid phase transition at 745 K ($\Delta_{trs}H_m^0$=10.6 kJ mol^{-1}) and decomposes peritectically at 759 K. The eutectic composition, $x(TbBr_3)$=39.5 mol%, was determined by the Tamman method. This eutectic mixture melts at 699 K with the corresponding enthalpy of about 16.1 kJ mol^{-1}. For the first time, the specific electrical conductivity of the liquid $TbBr_3$–NaBr mixtures as also that of pure $TbBr_3$ was determined and fitted by a quadratic function of the temperature.

* * *

Part of us (LR, EIS, MCG) acknowledges support from the Polish Committee for Scientific Research under the Grant 3 T09A 091 18.
LR also wishes to thank the Institut des Systèmes Thermiques Industriels (IUSTI) for hospitality and support during this work.

References

1 V. S. Naumov, A. V. Bychkov and V. A. Lebedev, Advances in Molten Salts: from structural aspects to waste processing, M. Gaune-Escard (Ed.) Begell House Inc., (1999) 432.
2 M. Kuroda and Y. Sakamura, J. Phase Equilib., 22 (2001) 232.
3 W. Van Erk, Pure Appl. Chem., 72 (2001) 2159.
4 M. Gaune-Escard and J. Fuller, High Temp. Mat. Proc., 3–4 (2001) 309.
5 M. Gaune-Escard, L. Rycerz, W. Szczepaniak and A. Bogacz, J. Alloys Comp., 204 (1994) 193.
6 M. Gaune-Escard, L. Rycerz, W. Szczepaniak and A. Bogacz, J. Alloys Comp., 204 (1994) 189.
7 M. Gaune-Escard, A. Bogacz, L. Rycerz and W. Szczepaniak, Thermochim. Acta, 236 (1994) 59.
8 M. Gaune-Escard, A. Bogacz, L. Rycerz and W. Szczepaniak, Thermochim. Acta, 236 (1994) 67.
9 M. Gaune-Escard, L. Rycerz and A. Bogacz, J. Alloys Comp., 204 (1994) 185.
10 R. Takagi, L. Rycerz and M. Gaune-Escard, Denki Kagaku, 62 (1994) 240.
11 M. Gaune-Escard, L. Rycerz, W. Szczepaniak and A. Bogacz, Thermochim. Acta, 236 (1994) 51.

12 M. Gaune-Escard, L. Rycerz, W. Szczepaniak and A. Bogacz, Thermochim. Acta, 279 (1996) 1.
13 M. Gaune-Escard, L. Rycerz, W. Szczepaniak and A. Bogacz, Thermochim. Acta, 279 (1996) 11.
14 M. Gaune-Escard, L. Rycerz and R. Takagi, J. Alloys Comp., 257 (1997) 134.
15 M. Gaune-Escard and L. Rycerz, V-th Int. Symp. on Molten Salt Chemistry and Technology, Dresden, Germany, 24–29 August 1997, Molten Salt Forum, v. 5–6 (1998) 217.
16 M. Gaune-Escard and L. Rycerz, Z. Naturforsch., 54a (1999) 229.
17 L. Rycerz and M. Gaune-Escard, Z. Naturforsch., 54a (1999) 397.
18 L. Rycerz and M. Gaune-Escard, The International George Papatheodorou Symposium, Patras, September 17–18, 1999, Proceedings, p. 95-99.
19 F. Da Silva, L. Rycerz and M. Gaune-Escard, Z. Naturforsch., 56a (2001) 647.
20 F. Da Silva, L. Rycerz and M. Gaune-Escard, Z. Naturforsch., 56a (2001) 653.
21 L. Rycerz and M. Gaune-Escard, Z. Naturforsch., 56a (2001) 859.
22 P. Gaune, M. Gaune-Escard, L. Rycerz and A. Bogacz, J. Alloys Comp., 235 (1996) 143.
23 K. Fukushima, T. Ikumi, J. Mochinaga, R. Takagi, M. Gaune-Escard and Y. Iwadate, J. Alloys Comp., 260 (1997) 75.
24 M. Gaune-Escard, L. Rycerz and A. Potapov, Sixth Int. Conf. on Molten Salt Chem. and Technology, Shanghai, China, October 8–13, 2001, Proceedings, p. 122.
25 A. K. Adya, R. Takagi and M. Gaune-Escard, Z. Naturforsch., 53a (1998) 1037.
26 M. Gaune-Escard, F. Da Silva, L. Rycerz, Y. Iwadate and A. K. Adya, Proc. Eleventh Int. Symp. on Molten Salts, XI, Electrochem. Soc. Inc., Pennington, 98–11 (1998) 627.
27 R. Takagi, F. Hutchinson, P. A. Madden, A. K. Adya and M. Gaune-Escard, J. Phys. Cond. Matt., 11 (1999) 64.
28 M. P. Tosi, Molten Salts/ from Fundamentals to Applications, M. Gaune-Escard Ed., Kluwer Academic Publishers, 2002, p. 1.
29 F. Da Silva and M. Gaune-Escard, Advances in Molten Salts: from structural aspects to waste processing, M. Gaune-Escard (Ed.) Begell House Inc., (1999) 125.
30 M. Sakurai, R. Takagi, A. A. Adya and M. Gaune-Escard, Z. Naturforsch., 53a (1998) 655.
31 Y. Fouque, M. Gaune-Escard, W. Szczepaniak and A. Bogacz, J. Chim. Phys., 75 (1978) 360.
32 G. J. Janz, Materials Science Forum, 73–75 (1991) 707.
33 R. E. Thoma, The Rare Earh Halides, in L. Eyring (Ed.), Progress in the Science and Technology of the Rare Earths, Pergamon Press, New York 1996, p. 90.
34 A. B. P. Lever, Inorganic Electronic Spectroscopy, 2nd edition, Elsevier, Amsterdam 1984.